NONLINEAR BUCKLING ANALYSIS OF HEMISPHERICAL SHELLS AS A RESPONSE TO LOADING EFFECTS WITH PARAMETRIC STUDIES ON THICKNESS AND SHALLOWNESS

KUMIL ALI

CIV531 TERM PAPER

5/17/22

Abstract

Shell structures are curved outer membranes that can cover large areas and maintain their shape without the need for frames. Shell structures have a variety of applications in mechanical, aerospace, and structural engineering, and with rapid developments towards curved-based design, the need for curved, folded and shell designs have expanded. In our study we sought to understand the critical buckling load for a hemispherical shell with a vertical downwards point force on the pole. This procedure was repeated for 9 shell configurations accounting for 3 different thicknesses and 3 distinct shallowness angles. Performing computations in FEA software ABAQUS, geometry, forces and boundary conditions could be modeled with tetrahedral elements. The required eigenvalues were obtained and multiplied by the reference load to obtain critical buckling loads and their respective buckling mode. From these results it was found that an increase in either thickness and/or shallowness angle generally increased the critical buckling load of the shell. As can be seen in the provided, however, many issues were visualized within the buckling modes. Efforts were then put into solving similar problems in the case of shells within arc geometries, and similar trends with thickness, and critical buckling were realized. Even with this simplification, unfortunately, the same issues in the buckling modes were still prevalent in the ABAQUS models.

TABLE OF CONTENTS

1. INTRODUCTION

While not necessary in every case within Civil Engineering, nonlinear structural analysis methods are important in obtaining a closer understanding of many real-life structures in comparison to normal linear analysis. Due to the need for higher accuracy or novel geometries, nonlinear analysis utilizes more advanced problem-solving methods within the finite element formulation. One such novel geometry that is applicable to civil engineering is the hemispheric shell. Defined as a shell structure forming a dome-like shape, these structures can be used to sustain pressure or other loading types. A hemispheric shell problem can be approximated with linear methods, to mixed results. To obtain more accurate results for important structural properties used in design, notably critical buckling load, nonlinear methods of analysis may be used.

To solve these structures, the popular finite element analysis software ABAQUS will be used. The geometry of the structure will be adapted to ABAQUS, and a buckling load analysis will be done for a vertical downwards point load at the top of the structure. The geometric parameters of thickness and shallowness will be adjusted so that multiple configurations of hemispheric shells can be analyzed. By adjusting these parameters, conclusions can be drawn about the effects of thickness and shallowness on buckling loads, as well as if there are any additive effects caused by the alteration of both properties.

Additionally, analysis of arc-like shells will be conducted similarly to the hemispheric shells. Results from this analysis will then be compared to that of the hemispheric shells to confirm validity in their solutions.

2. LITERATURE REVIEW

2.1 Nonlinear Analysis of Shells

Some time was spent on the theory of analysis of shells to properly determine what types of element selections to make for analysis. In general cases, shell theories depend on the assumption that the shell structure is thin. Because of this, simplifications to the 2-D plane can be made, with the appropriate simplifications. With a shell assumed to have a small thickness in comparison to its other geometric characteristics, transverse stresses and strains can be neglected. (Palazotto & Dennis, 1992) However, as this assumed thickness is increased, these transverse effects increase, especially in the case of shear. In such cases, approximations to thin shells may incorrectly characterize the problem. When performing an analysis of shells with multiple configurations of various thicknesses, as is the case in this report, the element type chosen may affect the adequacy of the produced critical load. Because of the variation in thickness between elements, general-use 3D elements were used in the place of ABAQUS thin shell elements. The use of these standard 3D elements may induce some changes when compared to thin shell element approximations.

2.2 Buckling Loads of Hemispherical Shells

Some studies were reviewed to help in the development of the project and to assist with interpreting results. Many articles discussing the buckling loads of hemispheric shells focus on cases with the applied force represented as a pressure, an equally distributed uniform surface force on the entire structure. While this may differ from the proposed singular downward force on the top of the shell as in our case, similar principles may apply.

Previous research by Koiter in the 1960s outlined what would later become a design code for the elastic strength of thin hemispheric shells. Under cases of externally applied pressures, such hemispheric domes would undergo experimental buckling loads that were as little as 20% of the load predicted for the structure utilizing other analysis methods, due to the presence of small imperfections in the real-life structures. (Hutchinson, 2016) Hutchinson re-approaches these ideas with new methods of nonlinear dynamics present in the current era to better understand the causes for this lower limit. Axisymmetric buckling, like what should be the case for hemispheric shells, is governed by nonlinear ODEs. As discussed in the article, the principles established by Koiter did not have the backing of numerical analysis codes in the 1960s, and thus there was no non-linear analysis of hemispheric shells which could accurately capture axisymmetric buckling. By utilizing moderate rotation theory, Donnell–Mushtari–Vlasov theory, and exact first order theory, Hutchinson can validate the experimental results of a 20% buckling load among other conclusions. Relevant to our experiment is the conclusion that a perfect shell will produce a localized non-uniform buckling deflection right after buckling occurs, which is quite different from the classic buckling mode.

In 2017 a study performed by Marthelot sought to determine a buckling load of a hemispheric shell due to a combination load of internal pressure and a probing force. (Marthelot, Jiménez, Lee, Hutchinson, & Reis, 2017) This study, therefore, is useful in drawing conclusions of our model subjected to only the force. In the first study conducted, a probing force is applied, and the internal pressure of the shell is gradually reduced to the point where the shell buckles. The second case, which is comparable to our experiment, involves establishing a reduced internal pressure of the shell and then increasing the value of the probing force to determine the buckling load. The 2017 study then solved for the buckling loads both experimentally (with a controlled geometric defect at the pole) and with FEM formulation. For the purposes of simulating this defect in FEM software, changes were made to the shell for a small indentation at the pole in the direction of the probing force. Due to this geometric defect located at the pole, and due to the point load being at this defect, it was found that the experimental results coincided with the simulated results.

In our own experiment there would be no difference in pressure between the outside surface and inside surface of our shell. Additionally, we would be assuming the analysis of a perfectly symmetric shell with no defects at all. Either of these assumptions could be expected to produce differing results from what was found in Marthelot's research and may be the cause of issues later in our methodology/results. In combination with the change of element choice, different behaviors entirely may be produced.

3. METHODOLOGY

The overall procedure to develop a hemispherical shell involves determining the overall geometry to vary the shallowness regimes. To begin, a part must be defined, with options being given for the 3D modelling space and the definition of our shell structure. Defining these conditions allows us to determine an ideal shape with special considerations given for its shallowness regimes. Our base shape was a 500 mm radius circle for our standard regime, our super-shallow regime required a 500mm x 1000 mm ellipse, and our steep regime required a 500 mm x 200 mm ellipse.

To perform a non-linear analysis of a hemispheric shell, FEA software ABAQUS was used. There would be nine total shell configurations, encompassing 3 different thicknesses and three different shallowness cases. All the above configurations would feature the isotropic conditions in material, an elastic modulus of 190 GPa, and a Poisson's ratio of 0.3. An Elastic Modulus of 190 GPa was chosen to represent a soft-deformable steel, these properties simulate steel types commonly used in civil engineering applications. Table 1 contains all configurations sets used in analysis.

Table 1: All Configuration Cases

Configuration	Shallowness Angle	Thickness (mm)
1	45	1
2	45	50
3	45	250
4	90	1
5	90	50
6	90	250
7	145	1
8	145	50
9	145	250

In our model, for each shallowness and thickness regime, our bottom and lower edges were constrained to prevent movement in the x- and y- and z- directions. We wanted to prevent movement in these directions to allow for the determination of a static critical buckling load of the shell as well as its mode. A reference load of 1 N was applied downward from the pole of our hemispherical shell. Figure 1 attached indicates the boundary conditions and loads applied. The reference load can simply be multiplied by the ABAQUS-produced eigenvalue to determine the critical buckling load and mode of each shell configuration. Therefore, this would mean that any force lower than the acquired buckling would be resisted by the structure without collapse failure. As previously stated, general elements would be used for all configurations. In ABAQUS, the described element is 4-noded linear tetrahedron, or C3D4 element. Due to software limitations in the student version of ABAQUS, we were limited to a total of 1000

elements. For each structural configuration, various trials were conducted to cap the number of elements discretized to upper limit to minimize overall variability in our models.

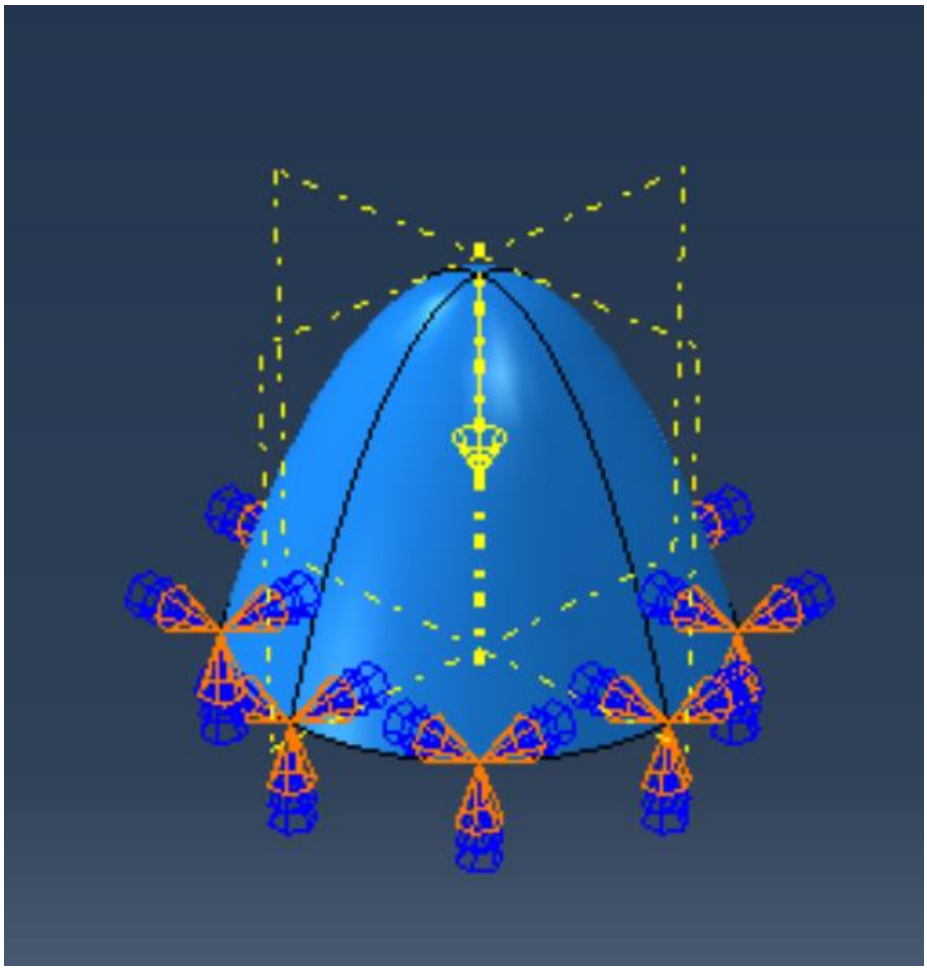

Figure 1 Boundary and Loading Conditions applied

4. DISCUSSION OF RESULTS

The aforementioned methodology was implemented and used for the development for the 3D FEA simulations of the hemispheric shell structure. All the parameters were then applied to the arc-shell structures which were simply linear cuts from their respective hemispheric shell predecessor. After developing the geometry and results in the form of the first buckling modes and the associated values were obtained and can be seen in the figures provided in the section.

4.1 Hemispheric Shell Buckling Load

The primary purpose of our project was to determine the critical buckling loads and the first buckling loads for the suggested configurations of both thickness and shallowness. What can be seen in the screenshots produced from ABAQUS is the solid along with a heatmap containing the displacement magnitudes of the discretized nodes of the structure.

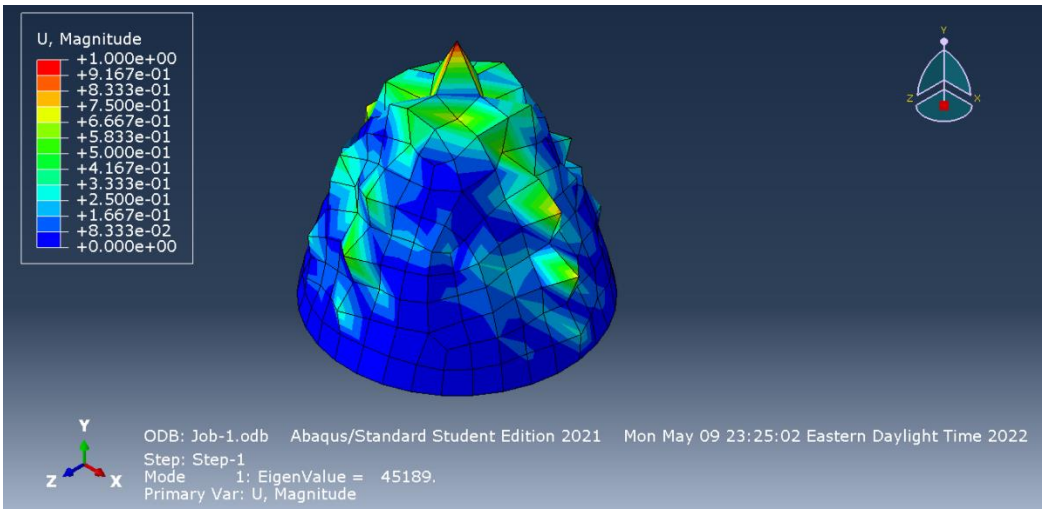

Figure 2 Buckling Load Analysis of Configuration 1: 45 degrees, 1 mm thickness

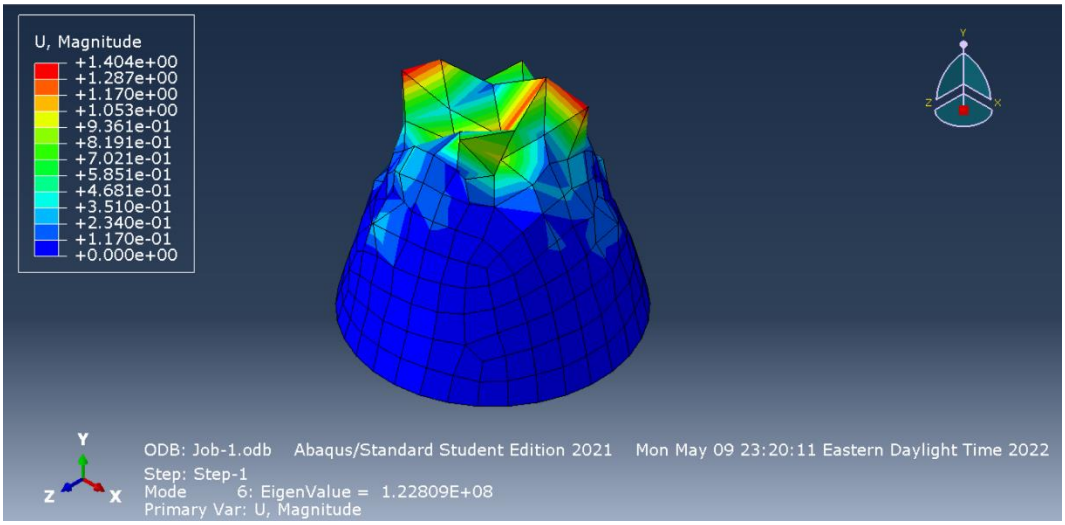

Figure 3 Buckling Load Analysis of Configuration 2: 45 degrees, 50 mm thickness

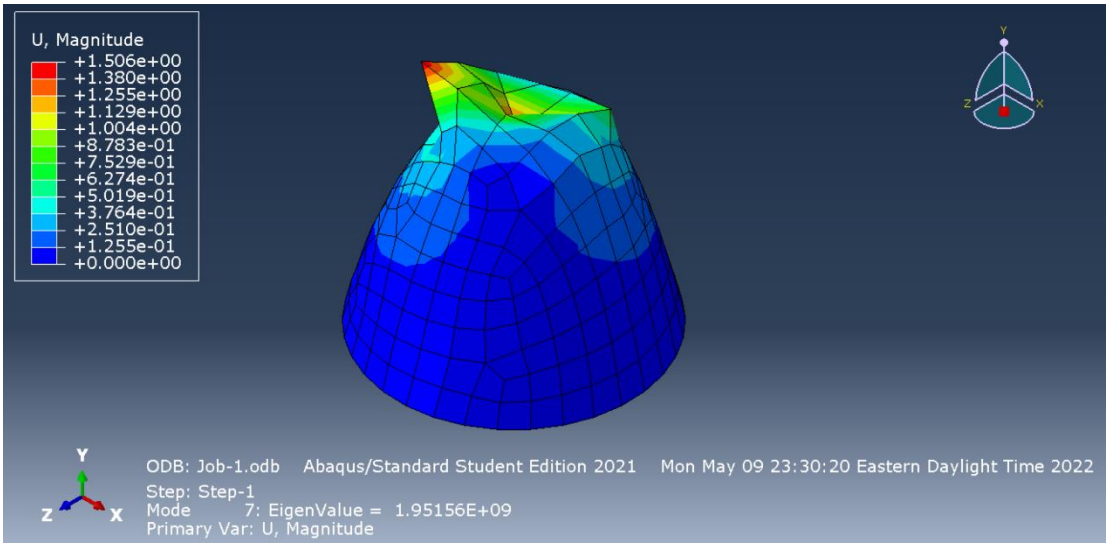

Figure 4 Buckling Load Analysis of Configuration 3: 45 degrees, 250 mm thickness

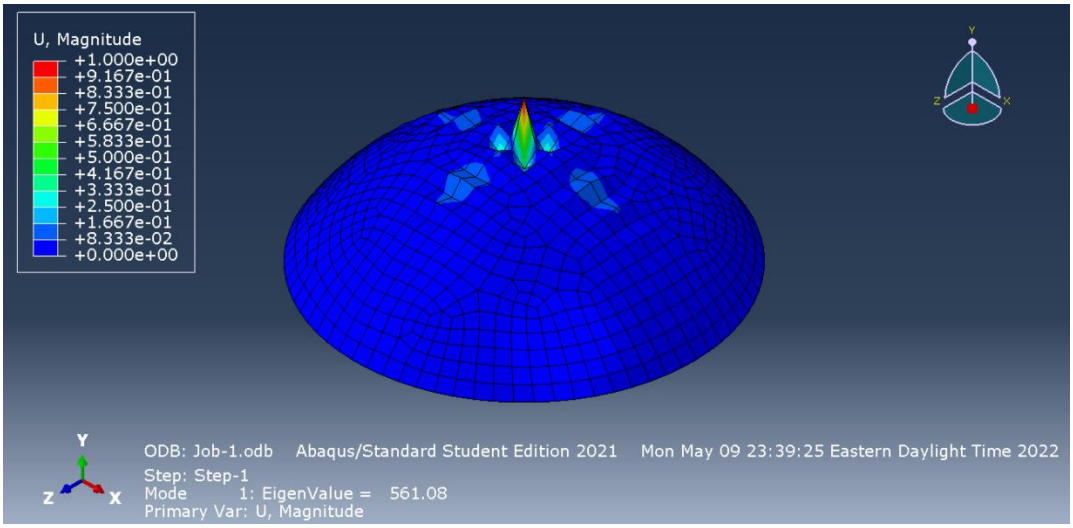

Figure 5 Buckling Load Analysis of Configuration 4: 90 degrees, 1mm thickness

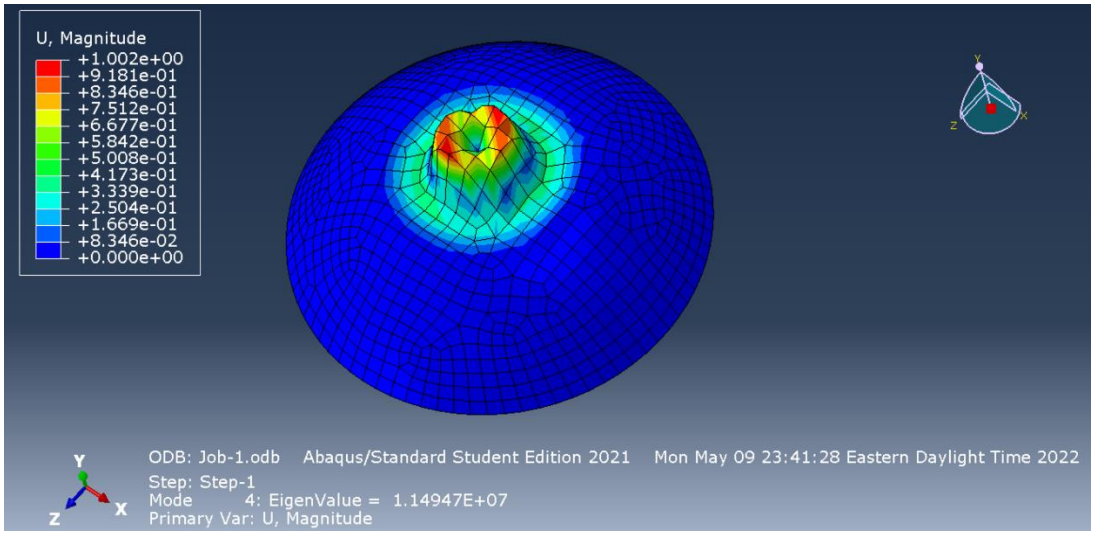

Figure 6 Buckling Load Analysis of Configuration 5: 90 degrees, 50 mm thickness

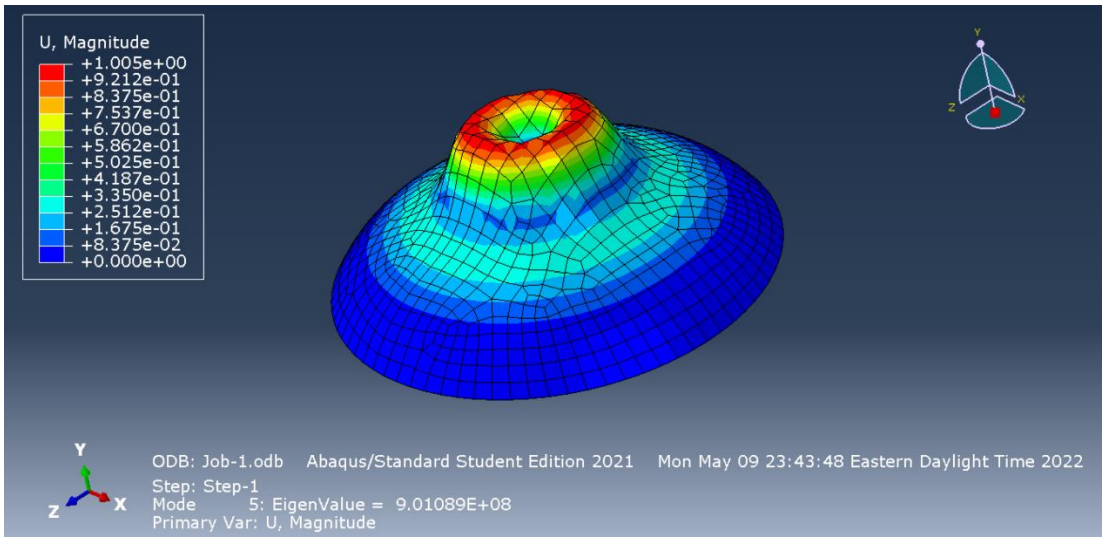

Figure 7 Buckling Load Analysis of Configuration 6: 90 degrees, 250 mm thickness

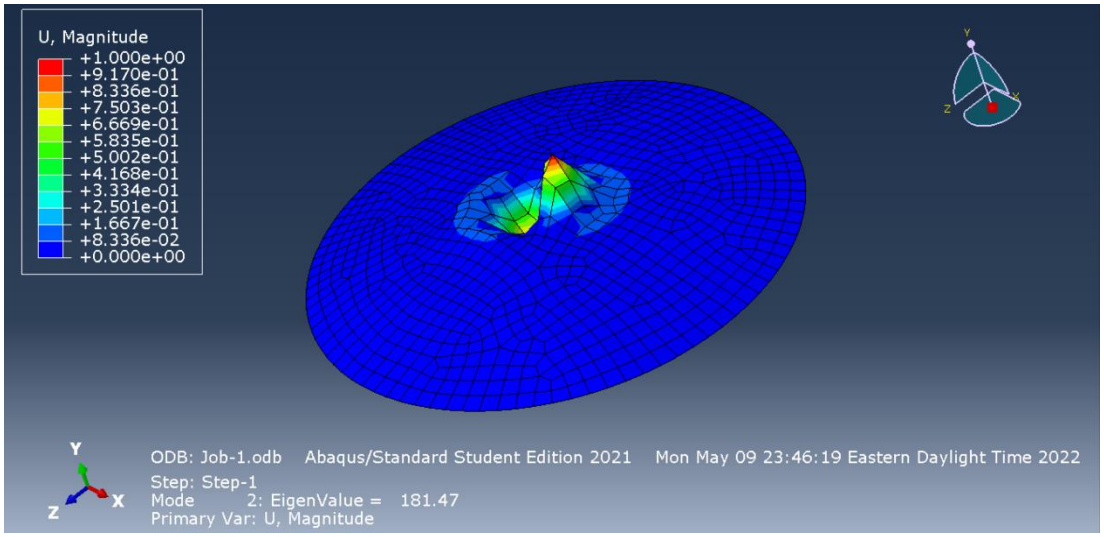

Figure 8 Buckling Load Analysis of Configuration 7: 145 degrees, 1 mm thickness

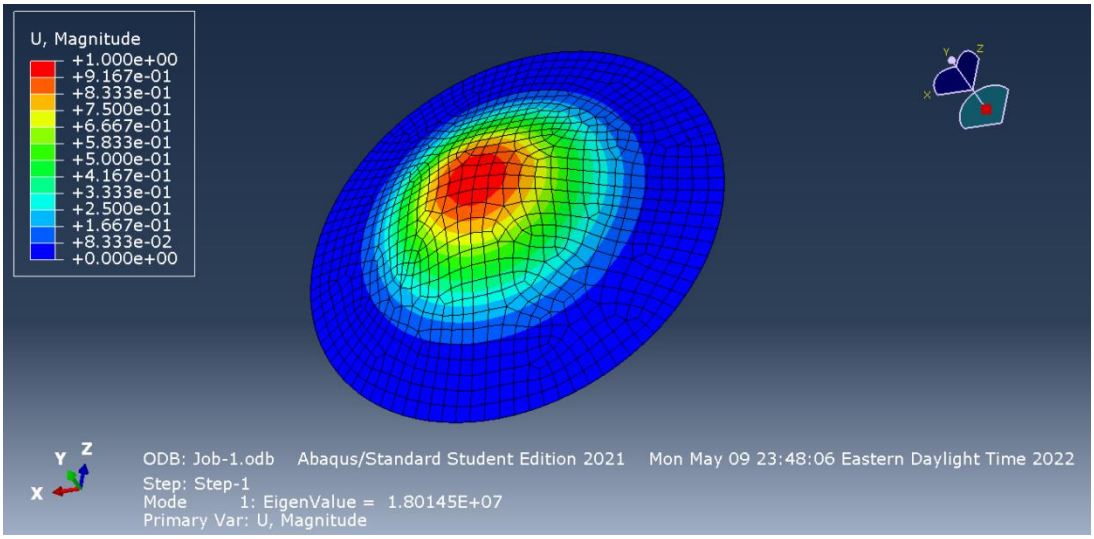

Figure 9 Buckling Load Analysis of Configuration 8: 145 degrees, 50 mm thickness

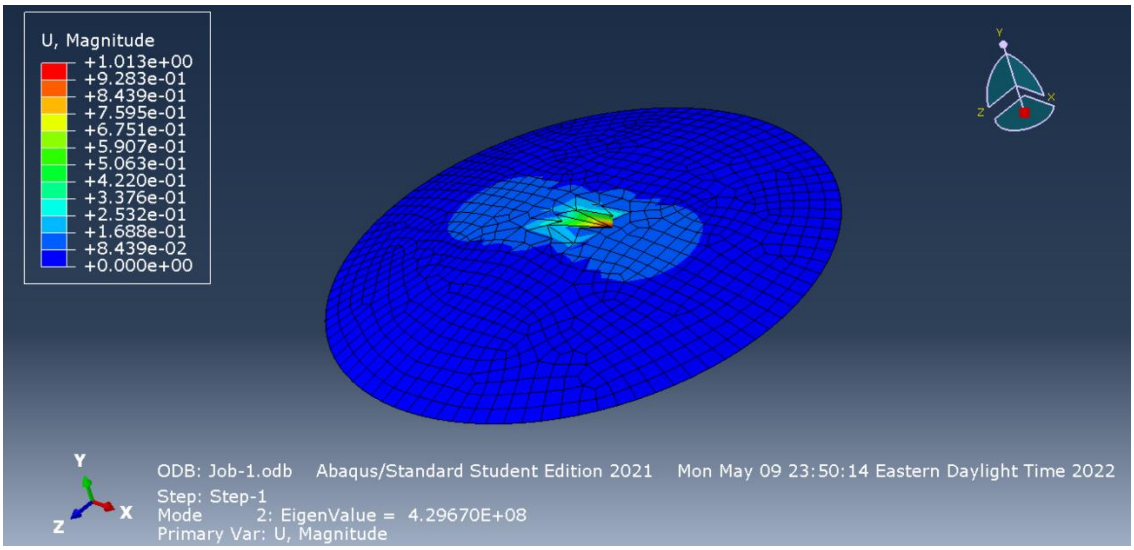

Figure 10 Buckling Load Analysis of Configuration 9: 145 degrees, 250 mm thickness

Table 2 Critical Buckling Loads for Hemispheric Shell Configurations

Shallowness	Thickness (mm)	Eigenvalue	Critical Buckling Load (N)
Steep	1	45189	45189
Steep	50	$1.22x10^8$	$1.22x10^8$
Steep	250	$1.95x10^9$	$1.95x10^9$
Standard	1	561.08	561.08
Standard	50	$1.15x10^7$	$1.15x10^7$
Standard	250	$9.01x10^8$	$9.01x10^8$
Super Shallow	1	181.47	181.47
Super Shallow	50	$1.80x10^7$	$1.80x10^7$
Super Shallow	250	$4.29x10^8$	$4.29x10^8$

Our models generated various mode shapes and eigen-values, and due to the variability in our model with the number of elements, it was decided to find 10 eigen-values for each configuration. The lowest eigen-value was then selected to compute the critical buckling load. General trends produced the expected results, at least for relative comparisons between configurations. Thicknesses prove a large part of the critical buckling load of the structure, and higher thicknesses result in higher critical buckling loads. Similarly, increasing progression in shallowness produces the same higher the critical buckling for a given thickness, apart from the change from steep 1mm to standard 1mm.

However, the captured behavior of our models were hard to align with the principles learned in class and in the literature. Given our placement of a reference load, we would assume that our shells would display an indentation where the load was applied and deform gradually from the application of the concentrated load on the structure; configurations with greater thickness should show lower overall deformation from the point of contact of the force on the

structure. Our buckling shapes did not show behavior that was holistically accepted, and the modifications of shallowness for each structure generated complex and unique results. One key aspect to consider would be that our models did display indentation under the application of the concentrated load, but in an entirely different direction displaying a pop-up effect. Experimentation with changing the loading direction still produced the same buckling shapes, but with negative eigenvalues. Overall, we do capture some of the effects included in the different configurations, but a combination of the factors differentiating our project from (Marthelot, Jiménez, Lee, Hutchinson, & Reis, 2017) may have led to these less-than-stellar visualizations.

4.2 Arch Shell Buckling Load

After troubleshooting and discussion with the course professor, it was proposed to simplify the problem further into an arc-shaped shell. This was done through cutting the preexisting shell configurations into these strips like structures, with identical material, boundary, and loading conditions. The hopes for these new configurations was that more predictable behavior would be determined and applied to the hemispherical shells.

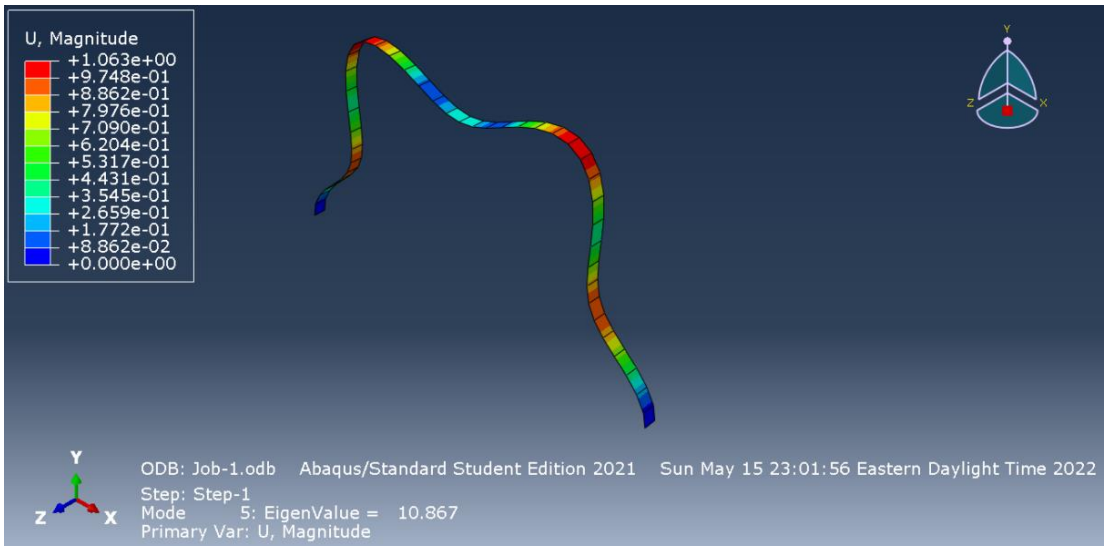

Figure 11 Buckling Load Analysis of Arch Standard Configuration 1: 45 degrees, 1 mm thickness

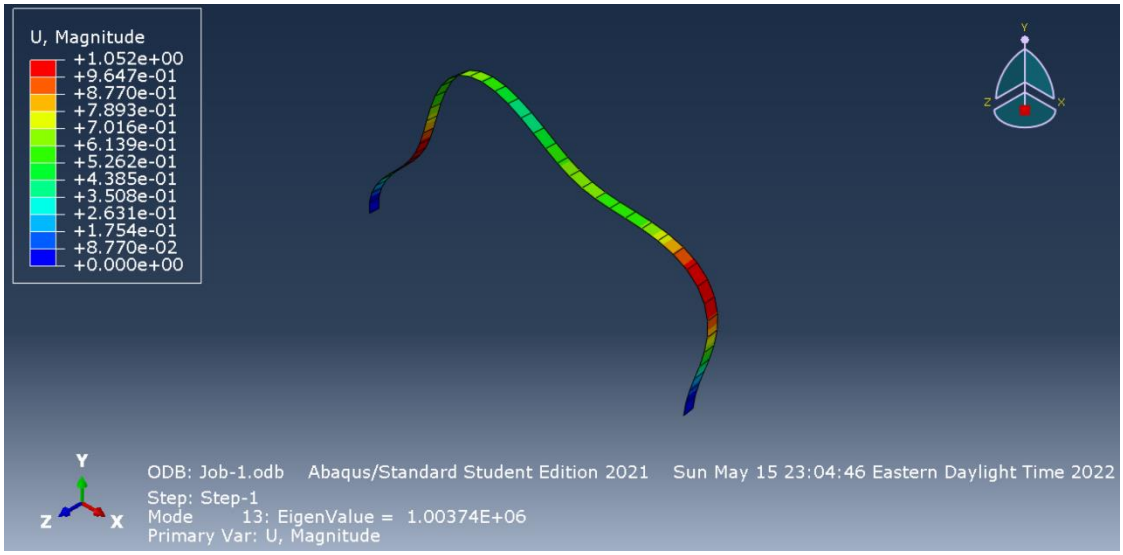

Figure 12 Buckling Load Analysis of Arch Standard Configuration 2: 45 degrees, 50 mm thickness

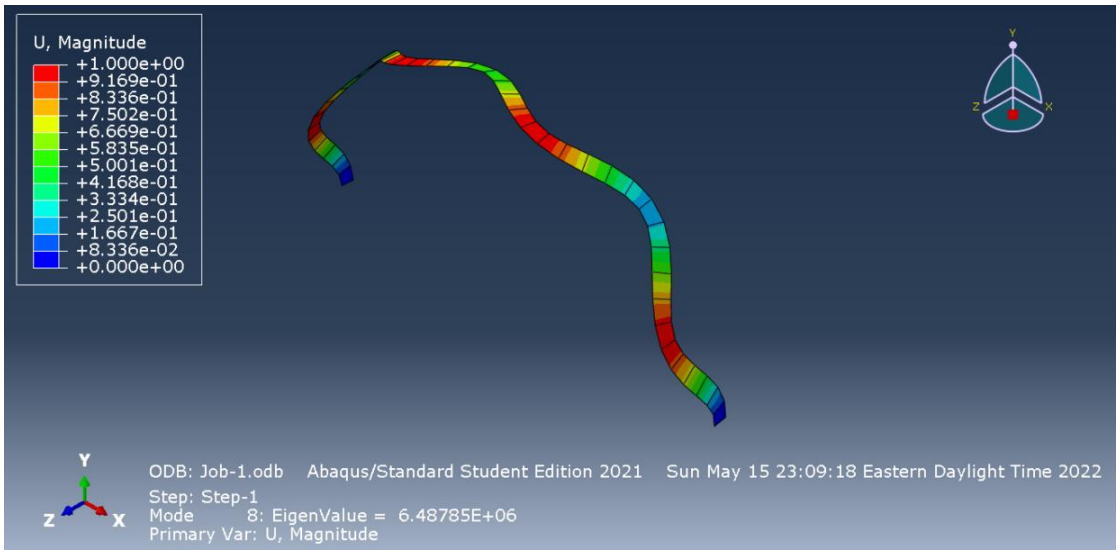

Figure 13 Buckling Load Analysis of Arch Standard Configuration 3: 45 degrees, 250 mm thickness

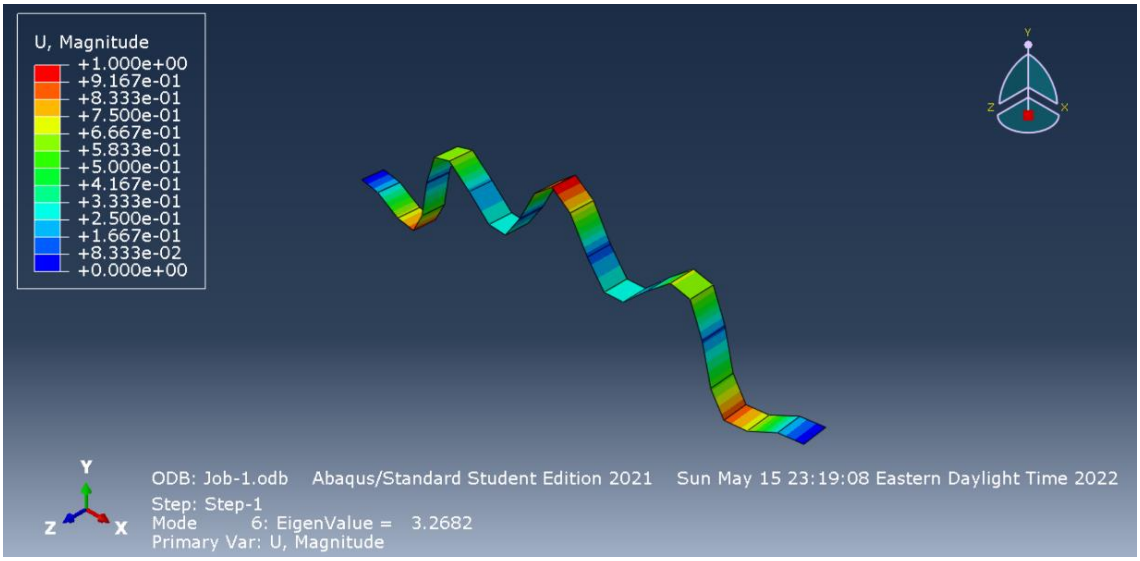

Figure 14 Buckling Load Analysis of Arch Standard Configuration 4: 90 degrees, 1 mm thickness

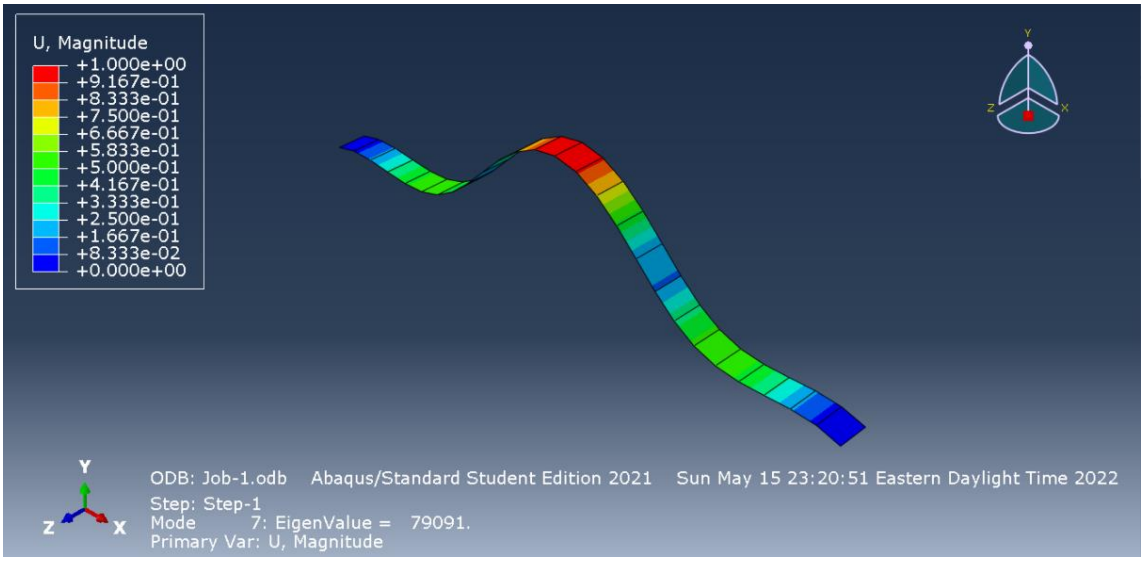

Figure 15 Buckling Load Analysis of Arch Standard Configuration 5: 90 degrees, 50 mm thickness

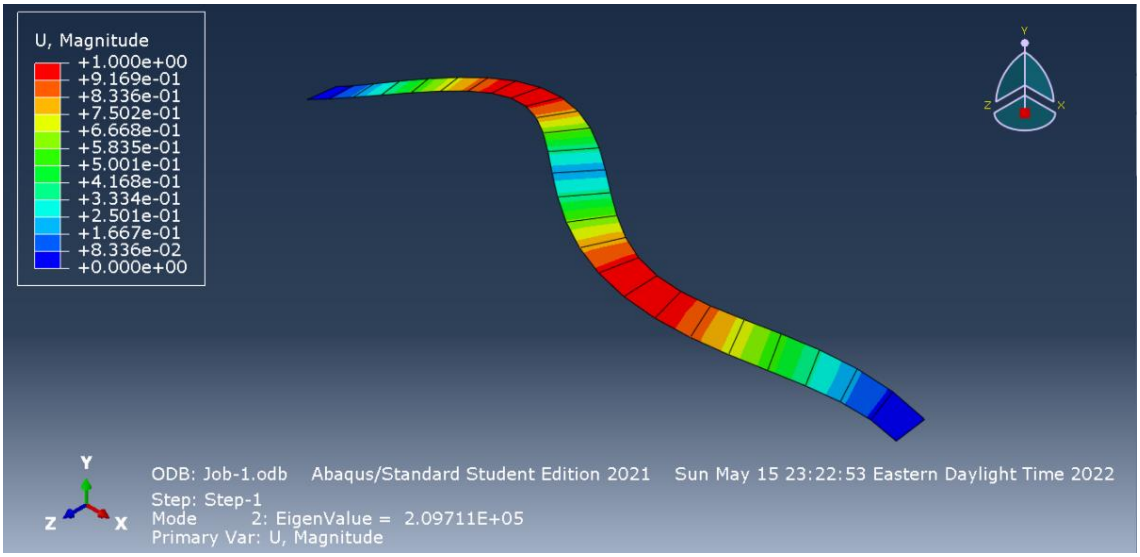

Figure 16 Buckling Load Analysis of Arch Standard Configuration 6: 90 degrees, 250 mm thickness

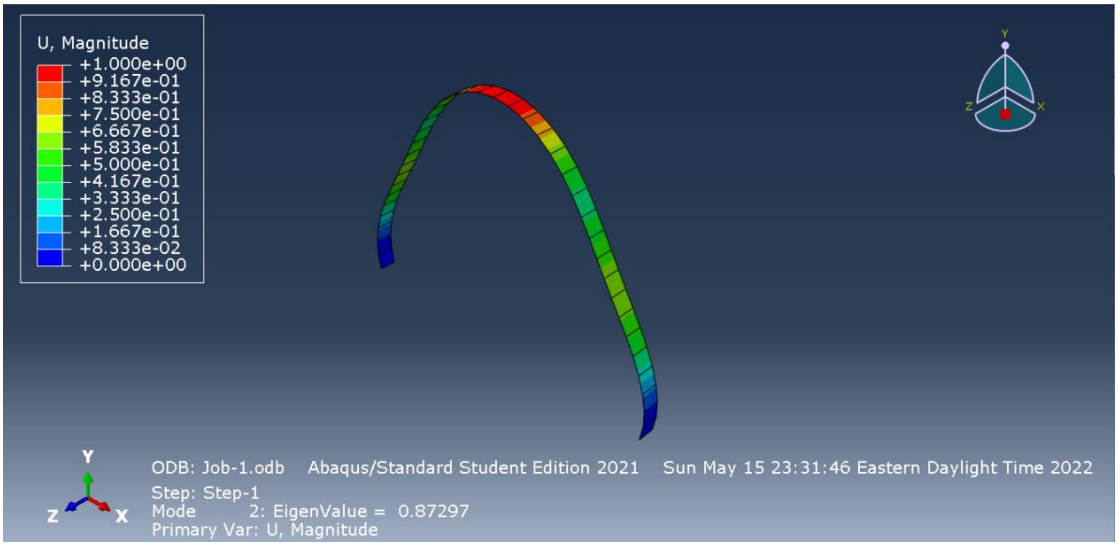

Figure 17 Buckling Load Analysis of Arch Standard Configuration 7: 145 degrees, 1 mm thickness

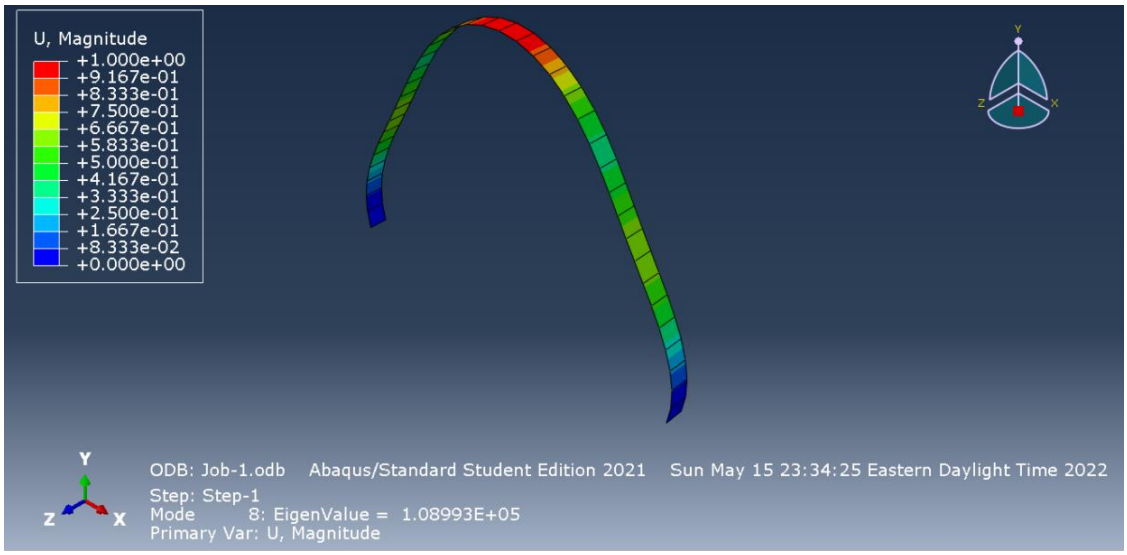

Figure 18 Buckling Load Analysis of Arch Standard Configuration 8: 145 degrees, 50 mm thickness

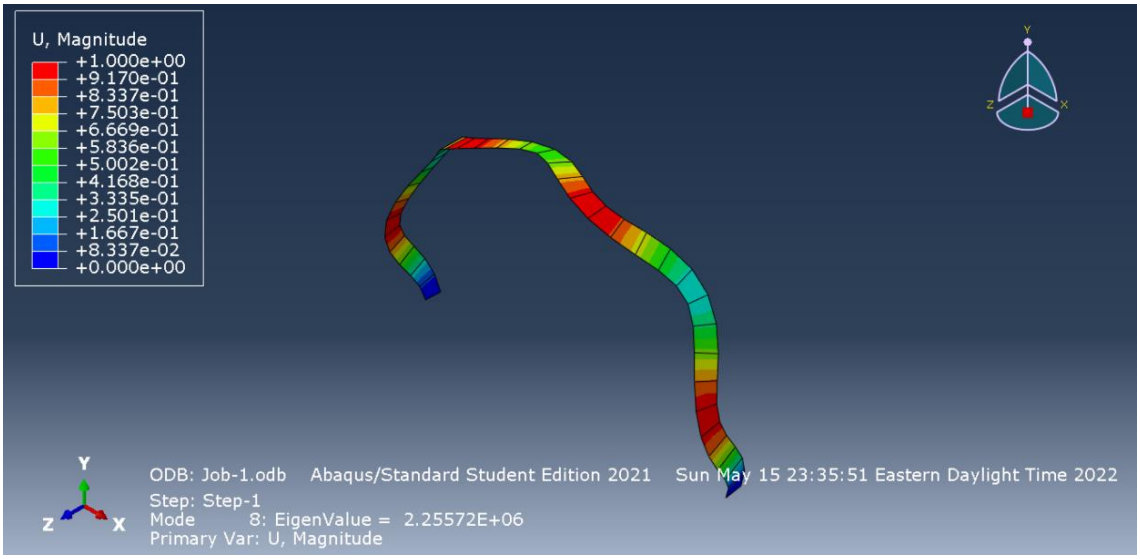

Figure 19 Buckling Load Analysis of Arch Standard Configuration 9: 145 degrees, 250 mm thickness

Table 3 Critical Buckling Loads for Arch Shell Configurations

Shallowness	Thickness (mm)	Eigenvalue	Critical Buckling Load (N)
Steep	1	0.872	0.872
Steep	50	1.08×10^5	1.08×10^5
Steep	250	2.26×10^6	2.26×10^6
Standard	1	10.87	10.87
Standard	50	1.00×10^6	1.00×10^6
Standard	250	6.49×10^6	6.49×10^6
Super Shallow	1	3.27	3.27
Super Shallow	50	7.91×10^4	7.91×10^4
Super Shallow	250	2.10×10^5	2.10×10^5

Observing the trends in critical buckling loads for each configuration, the general trends of an increasing critical load for an increasing thickness. In the case of shallowness, any trends among an increasing shallowness angle are questionable. Through visual observations of the undeformed structure, it should be a given that there would be better, although that was not the case in every instance. For example, comparing Figure 18 and Figure 19 are really only different in thickness, but portray vastly different critical buckling modes, with Figure 19 even deforming in additional directions.

5. CONCLUSION

By using a limit of 1000 standard 3D elements, a perfect hemispherical shell, and vertical force on that hemispherical shell's poll, eigenvalues and therefore critical buckling loads were determined. Experimental studies were used as background information and to help produce conclusions about our model. For the nine configurations of hemispherical shells used, there were general trends of an increasing buckling loads because of both increasing thicknesses and increasing shallowness angles.

What could be seen from the given methodology was that unique and unexpected visualizations of the structure's buckling modes were hard to describe in any analytical manner. As a potential solution for these issues, the procedure was repeated for similarly defined arc shells, to simpler but still anomalous results. Future work in this project could utilize other element types, such as higher element counts, or different element types. ABAQUS shell elements, for example, could be used and compared with the standard tetrahedron elements used in this report.

6. REFERENCES

Chapelle, D., & Bathe, K.-J. (2011). *The Finite Element Analysis of Shells- Fundamentals 2nd Edition.* Berlin: Springer.

Hutchinson, J. W. (2016). Buckling of Spherical Shells Revisited. *Proc. R. Soc. A*, 472-497.

Marthelot, J., Jiménez, F. L., Lee, A., Hutchinson, J. W., & Reis, P. M. (2017). Buckling of a Pressurized Hemispherical Shell Subjected to a Probing Force. *Journal of Applied Mechanics 84(12)*, 121005-1 - 121005-9.

Palazotto, A., & Dennis, S. (1992). *Nonlinear Analysis of Shell Structures.* Washington DC: American Institute of Aeronautics and Astronautics.

Steigmann, D. (2013). Koiter's Shell Theory from the Perspective of Three-dimensional Nonlinear Elasticity. *Journal of Elasticity, Springer Verlag, 111 (1)*, 91-107.